Particle methods for 3D biological flows with variable density and viscosity

Robin Chatelin, Philippe Poncet

European Congress on Computational Methods
in Applied Sciences and Engineering (ECCOMAS 2012)
J. Eberhardsteiner et.al. (eds.)
Vienna, Austria, September 10-14, 2012

PARTICLE METHODS FOR 3D BIOLOGICAL FLOWS WITH VARIABLE DENSITY AND VISCOSITY

Robin Chatelin[1,2] *, **Philippe Poncet**[1,2]

[1]Toulouse Institute of Mathematics, CNRS, Team MIP. F-31077 Toulouse, France.
[2]Université de Toulouse, INSA, GMM 135 avenue de Rangueil, F-31077 Toulouse, France. address
robin.chatelin@math.univ-toulouse.fr, philippe.poncet@math.univ-toulouse.fr

Keywords: Particle methods, Three-dimensional flows, Stokes equations, Complex geometry, Variable density flows, Variable viscosity flows, Biological flows, Lung pathologies.

Abstract. *This work is investigating a mechanical dysfunction of human lungs: Mucociliary clearance. The goal is to understand how diseases like cystic fibrosis impact mucus motion (by altering mucus viscosity, cilia vibrations, respiration cycle...) and to identify stagnation situations where pathogens proliferate. Strategies for computation of mucus flow around an epithelium ciliated cell are presented. Governing equations are proposed to take into account this complex geometry in motion in the surrounding highly viscous fluid. The characteristic Reynolds number of the flow is very small and mucus is modelled by Stokes problem with both variable viscosity and density. Epithelium displacement is taken into account using a penalization method. As density and viscosity follow a convection equation, these assumptions lead to an elliptic/hyperbolic coupling and non-linear equations. Numerical implementations are discussed to get a fast, robust and accurate algorithm in three dimension based on fast elliptic solvers and Lagrangian methods.*

1 INTRODUCTION

In the lung a mucus film is covering the bronchial wall. It plays a role of barrier and traps inhaled dust, pollution chemicals and pathogen agents breathed. The mucus film is always moving from distal to proximal airways: it flows until ascending trachea to the commissure of larynx where it is swallowed in the gastrointestinal tract. This phenomenon is called mucociliary clearance and is absolutely necessary to avoid bacterial proliferation and infections of bronchial wall. Epithelium cells are covering bronchial walls and their cilia of about 6 to 10 μm long are beating at frequencies from 4 to 20 Hz to propel mucus film.

If mucus film is too thin and not viscous enough lung wall remains vulnerable to pathogens. Paradoxically if it is too viscous and too thick cilia are not able to propel it and stagnation regimes are observed: pathogens are proliferating and injuring lung. This overload of mucus in airways is notably a consequence of diseases like cistik fibrosis [9, 10]. Mucociliary clearance is based on a well balance of several physiological parameters of the lung which are very difficult to quantify since in vivo observations are very limited [10].

Mucus film is composed of two different fluids: mucus which is a highly viscous gel and periciliary fluid (PCF) which is hydrated and less viscous. The interface between both these fluids is not clearly identifiable since they are miscible (both composed of water) but flow parameters such as density and viscosity are strongly varying from PCF to mucus gel.

In this microfluidics context and with such viscosities (close to water's for PCF and increasing for mucus) Reynolds number is very small and diffusion is dominating advection so Navier Stokes equation are simplifying into Stokes problem. Classical Stokes problem is linear but variable viscosity is inducing a non-linearity since diffusion term does not reduce to a Laplacian. Stokeslet method based on fundamental kernel solution has been widely used for computation of Stokes problem around cilia [15] but this method needs to inverse linear systems to compute source forces, the support of fundamental Stokeslets based on Green function is wide so computation are very costly if they are used in an iterative process to add non-linearity. Moreover methods based on fundamental functions are complicated to implement with periodic boundary conditions since Green function support can overlap over several periods inducing wide summations. In the same way full discretisation of Stokes problem using finite elements, finite volumes or finite differences will impose the use of a very large matrix due to 3D computations, it is very long to assemble and resulting linear system is badly conditioned and does not enable to threat straightly the non-linearity.

In this context Stokes problem with spacial varying viscosity and incompressibility condition is coupled with a rheological law stating viscosity straightly depends on mass fraction [4]. This mass fraction is solution of an advection-diffusion equation where advection field is solution of Stokes flow.

Stokes conservation of momentum and incompressibility are solved using an iterative algorithm based on a projection method [11], an explicit treatment of non-linearity and a penalization method [2] for solid/fluid interaction. This enables to use fast 3D solvers. Numerical resolution of advection-diffusion is based on a splitting algorithm and hybrid particle/grid method [6, 7, 13] to avoid CFL restrictive condition and to guarantee good mass conservation.

In a first part modelling equations are presented and numerical strategies to solve the resulting coupled problem are discussed. Then an application is presented for computations of mucus flow around a single cilium and around a simplified cell described as an array of nine cilia and efficiency of mucociliary clearance is discussed.

2 EQUATIONS AND RESOLUTION ALGORITHM

This part is focusing on 3D equations used to model interactions of fluid-solid in a highly viscous regime with a variable viscosity and their numerical resolution. Fluid velocity will be denoted $u = (u_x, u_y, u_z)$. It is discretised on an Eulerian grid and Q is the computation box. Inside a solid is evolving with time and $B(t)$ denotes solid domain such that fluid domain reads $Q \setminus B(t)$.

In the highly viscous regime Navier-Stokes equations are reduced to Stokes problem which is quasi-static. The interaction with an immersed solid in this flow is taken into account with a penalization method [2]. Let introduce $\overline{u}(t)$ the velocity of solid body at instant t and $\chi(t)$ the characteristic function of solid domain $B(t)$.

Then coupled equation system for Stokes flow with advection-diffusion of mass fraction α, variable viscosity defined as a function of α and penalization is:

$$\partial_t \alpha + u \cdot \nabla \alpha - \eta \Delta \alpha = 0 \quad \text{in } Q \tag{1}$$

$$\mu(x,t) = \phi(\alpha(x,t)) \quad \text{in } Q \tag{2}$$

$$-\mathrm{div}\,(\tau) + \nabla p + \frac{\chi(t)}{\varepsilon}(u - \bar{u}) = f \quad \text{in } Q \tag{3}$$

$$\mathrm{div} u = 0 \quad \text{in } Q \tag{4}$$

$$u(x,t) = \vartheta(x,t) \quad \text{on } \partial Q \tag{5}$$

$$\frac{\partial \alpha(x,t)}{\partial n} = 0 \quad \text{on } \partial Q \tag{6}$$

With α the mass fraction, η the mass diffusion, ϕ the rheological law, u the fluid velocity, p the pressure, μ the viscosity, $\tau(u) = 2\mu D(u) = \mu\left(\nabla u + \nabla u^T\right)$ the strain rate tensor and ε a small penalization parameter.

Numerical resolution of the coupled problem is fully described in [5] and summarised in following section.

This equation system implies μ is defined as a function of mass fraction through rheological function ϕ. Thus viscosity is solution of a similar equation as α but with an extra term:

$$\partial_t \mu + u \cdot \nabla \mu - \eta \Delta \mu = -\eta \frac{\phi''(\alpha)}{\phi'(\alpha)^2} \|\nabla \mu\|_2^2 \quad \text{in } Q \tag{7}$$

Then if $\phi'' = 0$, μ and α are solutions of the same equation with identical homogen Neumann boundary conditions since $\frac{\partial \mu}{\partial n} = \nabla \mu \cdot n = \phi'(\alpha) \nabla \alpha \cdot n = 0$. If α is following a purely advection equation $\eta = 0$ so μ and α are also following the same advection equation even if $\phi'' \neq 0$. This is the case of classical Navier-Stokes continuity equation when ρ is advected.

2.1 Stokes momentum equation with constant viscosity

In this section let consider Stokes problem: equations (3)-(4)-(5) assuming constant viscosity μ (variable viscosity is considered at the end of this section), solid velocity $\overline{u}(t)$ and characteristic functions $\chi(t)$ are known. Under this assumptions $\mathrm{div}\,(\tau) = \mu \Delta u$.

To satisfy incompressibility equation a projection method based on Chorin and Temam algorithm was adapted. It consists in solving first equation (3) without pressure gradient and with boundary conditions (5): this is an Helmholtz equation and it is computed using Mudpack

solver [1]. Then a projector ζ is computed as solution of a Laplace equation with Fishpack solver [16, 17]. These solvers do not need any matrix assembling which is very costly for 3D simulations. Finally previous velocity is corrected. As reported in [11] this projection method is generating spurious velocity on the boundary and corrected velocity does not verify equation (5) anymore. For quasi static flows this error can be very large instead of unsteady flows where projection is often chosen incremental. Moreover for unsteady flows panel methods can be used [14], it consists in solving integrals equations on a neighbourhood of the boundary scaling as $\sqrt{2\mu\delta t/\rho}$, it leads to very fast computations as long as this layer is small. For quasi static viscous flows the Green kernel support fills the whole domain inducing very long convolutions.

Spurious velocity can be cancelled using implicit boundary conditions instead of (5) by deducting in this equation what is adding in the correction. This implicit correction has also to be performed for the penalization term to ensure $u = \overline{u}$ after correction.

The complete fixed-point algorithm is presented with subscript k.

0. Initialise algorithm with $\nabla\zeta_k = 0$, $k = 0$.

1. Solve Helmholtz problem (8) with modified boundary conditions (9) and denote u^*_{k+1} the result.

$$-\mu\Delta u^*_{k+1} + \frac{\chi(t)}{\varepsilon}(u^*_{k+1} + \nabla\zeta_k - \bar{u}) = f \quad \text{in } Q \tag{8}$$

$$u^*_{k+1}(x,t) = \vartheta(x,t) + \nabla\zeta_k \quad \text{on } \partial Q \tag{9}$$

2. Compute a new projector ζ_{k+1} as solution of Laplace problem (10)-(11).

$$-\Delta\zeta_{k+1} = -\mathrm{div}u^*_{k+1} \quad \text{in } Q \tag{10}$$

$$\frac{\partial\zeta_{k+1}}{\partial n} = u^*_{k+1}\cdot n \quad \text{on } \partial Q \tag{11}$$

3. Correct intermediate velocity u^* as $u_{k+1} = u^*_{k+1} - \nabla\zeta_{k+1}$.

4. Check convergence of the algorithm by controlling for example $\|u_{k+1} - u_k\| \leq \varepsilon$ and $\|u_{k+1|\partial Q} - \vartheta\| \leq \varepsilon$ and if it is not reached go to step 1 and increment k .

5. The velocity field solution of Stokes problem with penalization is $u = u_{k+1}$.

2.2 Variable viscosity

If viscosity is not homogen with respect to space, there is a non linear term to had to momentum equation since $\mathrm{div}\,(\tau) = \mu\Delta u + \left(\nabla u + \nabla u^T\right)\nabla\mu + \mu\nabla\mathrm{div}u = \mu\Delta u + \left(\nabla u + \nabla u^T\right)\nabla\mu$ using incompressibility. This rewriting enables to use the previous 5-steps algorithm by computing the linear part $\mu\Delta u$ without any change and the non linear part is threaten explicitly in right hand side. Thus equation (8) simply has to be replaced by equation (12)

$$-\mu\Delta u^*_{k+1}\nabla\mu + \frac{\chi}{\varepsilon}(u^*_{k+1} - \nabla\zeta_k - \bar{u}) = f + 2D(u^*_k) \quad \text{in } Q \tag{12}$$

This is a minor change in the algorithm and it adds another criterion in the fix point. Furthermore convergence of this criterion has been observed to be converging faster than criterion presented before so this change does not imply larger computations. See [5] for details of residuals and convergence rates.

2.3 Advection-diffusion of mass fraction

Let now consider the advection-diffusion equation for mass fraction. In this equation advection is more important than diffusion but no term can be neglected. An operator splitting is introduced to compute independently advection and diffusion. This splitting strategy enables to recover at least first order accuracy and it can be increased using various sub-steps strategies [3, 7, 13].

The complete system is the following with u the fluid velocity field which is solution of Stokes problem and computed with the algorithm described before.

$$\partial_t \alpha + u \cdot \nabla \alpha - \eta \Delta \alpha = 0 \quad \text{in } Q \tag{13}$$
$$\frac{\partial \alpha(t,x)}{\partial n} = 0 \quad \text{on } \partial Q \tag{14}$$
$$\alpha(0,x) = \alpha_0(x) \quad \text{in } Q \tag{15}$$

Splitting strategy consists in separating this problem in two easier problems. The first one is a purely advection problem and the second one is a purely diffusive problem.

$$\partial_t \alpha^c + u \cdot \nabla \alpha^c = 0 \quad \text{in } Q \tag{16}$$
$$\alpha^c(0,x) = \alpha_0^c(x) \quad \text{in } Q \tag{17}$$

$$\partial_t \alpha^d - \eta \Delta \alpha^d = 0 \quad \text{in } Q \tag{18}$$
$$\frac{\partial \alpha^d(t,x)}{\partial n} = 0 \quad \text{on } \partial Q \tag{19}$$
$$\alpha^d(0,x) = \alpha_0^d(x) \quad \text{in } Q \tag{20}$$

Then calling $\mathcal{A}^c(t)$ the operator associated to equation (16) such that $\alpha^c(t) = \mathcal{A}^c(t)\alpha_0^c$ and $\mathcal{A}^d(t)$ the operator associated to equation (18)-(19) such that $\alpha^d(t) = \mathcal{A}^d(t)\alpha_0^d$; the splitting strategy consists in discretising time over several time steps as $t_n = n\delta t$ and to state $\alpha(\delta t) = \mathcal{A}^d(\delta t)\mathcal{A}^c(\delta t)\alpha_0$ and recursively $\alpha(t_n) = (\mathcal{A}^d(\delta t)\mathcal{A}^c(\delta t))^n \alpha_0$.

Then discretisation of operators $\mathcal{A}^c$ and $\mathcal{A}^d$ can be discussed independently. Advection is computed using a Particle-in-Cell method and is solved explicitly. The diffusion is also computed explicitly because the small value of η does not impose very restrictive CFL conditions.

2.3.1 Particle-in-Cell method for advection

This section is focusing on the numerical strategy for solving equation system (16)-(17). Hybrid grid-particle algorithm introduced in [6, 7] is well adapted for transport equations because it transforms a partial differential equation into a set of ordinary differential equations. So that the associated CFL stability condition vanishes and it is possible to perform much larger time steps. No boundary condition is required for solving this equation it is implicitly defined by velocity field u.

To do so a Lagrangian discretisation of computation domain is performed on a set of K particles of volume v_k located at position ξ_k and holding a mass fraction α_k such that α is defined as a measure solution :

$$\alpha(t) = \sum_{k=1}^{K} \alpha_k(t) \delta_{\xi_k(t)} v_k \tag{21}$$

Equation set (16)-(17) can be rewritten as :

$$\frac{d\xi_k}{dt} = u(\xi_k(t), t) \tag{22}$$

$$\frac{d\alpha_k}{dt} = 0 \quad \text{and} \quad \frac{dv_k}{dt} = 0 \tag{23}$$

Particles volume stays constant because the advection flow u is a divergence free velocity field as a solution of Stokes equation. The right hand side of first equation is obtained computing the solution of Stokes quasi-static problem using μ as a function of α. As there is no CFL, large time steps can be performed and explicit methods are stable, thus assumptions made in previous section for computation of u are holding.

This hybrid method implies transfer between grid and particles. It is performed using an interpolation kernel Λ^ϵ constructed with Monaghan's kernel M'_4 [12]. This kernel has very good properties: it preserves firsts three moments of distributions, it is twice continuously differentiable (except in zero), it is symmetric and has a short compact support so that computations are becoming faster. Moreover this kernel has a spline like property $\sum_{k \in Z} M'_4(x + j) = 1$ which is ensuring good conservation. For example after particle transport, α can be recovered on the grid with the convolution:

$$\Lambda^\epsilon * \alpha(x) = \sum_{k=1}^{k=K} \Lambda^\epsilon(x - \xi_k) \alpha_k v_k \tag{24}$$

where convolution kernel is defined as the following rescaling, tensorialized on the three variables of space: $\Lambda^\epsilon(x) = \frac{1}{\epsilon^3} M_4'^{\otimes 3}(x/\epsilon)$.

Hybrid grid-particle methods convergence and consistence order is discussed in [6, 7, 13] in the context of unsteady Navier-Stokes equations solved with vortex method. This work is adapting such methods for Stokes-transport coupling, with velocity given as a solution of Stokes problem.

2.3.2 Mass diffusion

Computation of mass diffusion (18)-(19)-(20) is also performed explicitly, using classical second order finite difference stencil. As η is small the corresponding CFL condition is not restricting time steps. The boundary condition (19) ensures no mass is diffused outside of the domain.

The full algorithm using Runge Kutta 2 discretisation for transport equation leads to second order convergence rates with respect to both time and space. The use of M'_4 interpolation kernel is guaranteeing a good conservation of mass. Convergence, consistence, conservation and computation cost for our global problem are discussed with more details in [5].

3 BIOLOGICAL FLOW IN THE LUNGS

In this section simulations of a mucus film flow around an epithelium cell are presented. In the human lung mucus plays a barrier role which protects bronchial walls from inhaled dust and pathogen agents. Mucus is a highly viscous gel essentially composed of water, polymers and proteins. Among these proteins mucin play an important role: they are hydrophilic proteins released by goblet cells situated on bronchial walls so the film is hydrated at bottom whereas lung air flow is dehydrating the top of the film so it is less viscous at the bottom (where viscosity is very closed to water) than at the top (where it can be 10 to 10000 times more viscous with pathologies such as cystic fibrosis) [9]. In fact two fluid layers are constituting the film: close to bronchial wall this low viscous fluid is called periciliary fluid and mucus gel is above. Nevertheless both fluids are miscible and the interface is not identifiable and a variable viscosity with potentially large gradients is relevant to model this fluid.

Ciliated epithelium cells are located on the bronchial wall. Their cilia are immersed in mucus and beating at frequencies from 4 to 20 Hz. One cilium is 6 to 10 micrometers long with a radius of 100 to 500 manometers. A global displacement of a few centimetres per minute of mucus film has been observed [18]. So the characteristic Reynolds number of this flow is about 10^{-4} close to the wall and it is decreasing as viscosity is increasing.

Thus such Reynolds numbers are inducing the use of Stokes problem with variable viscosity transported by the flow and the use of algorithm described in previous sections is relevant. Interaction between cilia and fluid is taken into account using penalization so only the influence of solid on fluid is considered. This is so called a one-way solid-fluid interaction.

3.1 Cilia motion

Polymerisation of cilia is generated using a 1D partial differential equation posed along a parametrised curve of 3D space. Cilia are composed of a skeleton of nanotubes: there is usually a central pair of tubes surrounded by nine other pairs which are forming the cilia skeleton. Inside chemical reactions are responsible of polymerisation. Here the parametrised curve is describing the central skeleton of cilia and polymerisation effects are modelled by another advection equation which mimics very well cilia beating.

Let call $P(l,t)$ the curve position describing cilium at time t at a length l from cilium basis with $P :]0,1[\longrightarrow R^3$. L is the derivative of P with respect to l and a transport equation is posed on L:

$$\frac{\partial L}{\partial t} + v(t)\frac{\partial L}{\partial l} = 0 \tag{25}$$

Boundary conditions of this equation are naturally induced by the physics of the problem : $P(0,t) = 0$ ensures that cilia basis is not moving as it is built in bronchial wall and $L(0,t) = \frac{\partial P}{\partial t} = g(t)$ is generating an oscillating motion. This combination of boundary conditions induces that $P(1,t)$ is free to evolve. Stability of this problem is guaranteed by the positivity of transport field v.

Unconditionally stable Euler implicit method is used for temporal discretisation and backward finite difference schemes are used to discretize spatial derivatives since v is positive.

Problem is solved with unknown L and cilia is rebuilt at each time t with the relation (26). This model is not preserving the total length of cilium which can be recovered easily by formula (27): it allows elastic deformation of the parametrised curve.

$$P(l,t) = \int_0^l L(\lambda,t)d\lambda \tag{26}$$

$$L_{tot} = \int_0^1 \|\frac{\partial P}{\partial l}\|_2 dl = \int_0^1 \|L(l,t)\|_2 dl \tag{27}$$

An illustration of the resulting cilia motion is presented on figure 1. It is asynchronous such that cilia is not following the same path in recovery: going from right to left in blue (backward assuming trachea is in the positive x direction which is supposed to be the direction of net transport) than when it is in stroke in red (from left to right).

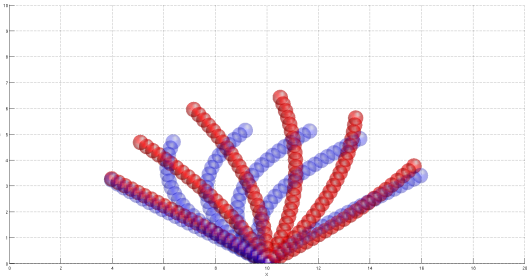

Figure 1: Trajectory followed by cilia motion. In blue are printed different instant when cilia is going from right to left (recovery), in red when it is coming back from left to right (stroke).

In the following simulation, motion of mucus is computed around one epithelium cell assuming periodic boundary conditions with respect to x and y directions. This states identical cells are located on the Oxy plane, beating in a coordinate manner. The curvature of the bronchial wall is neglected as computations are focusing on very small characteristic sizes. So that bottom plane of computation box is identified to bronchial wall inducing a no slip boundary conditions. At the top of the computation box mucus is authorised to displace in tangential direction: it is done using homogen Dirichlet boundary condition for u_z and Neumann boundary condition for both other components.

3.2 Simulation of mucus propulsion around a single cilium

A preliminary simulation of mucus flow around a single cilia is now presented. The different physical parameters used are synthesised in the following table. α is initialised as a linear function of the distance to bronchial wall while μ is a logistic function of α. Thus it has small gradients close to bottom and top of computation box while these gradients are more important in the region passing from periciliary fluid to mucus gel: region where cilia tips are passing during effective stroke and not during recovery. Simulation is performed over three beating periods and average velocity of film surface is under interest here to quantify efficiency of mucociliary clearance.

Beating frequency is $4\ Hz$ and each period is discretised by 50 time steps. These large time steps are inducing a large advection CFL number with a maximal value of 15. This means if a Lagrangian discretisation had not been used at least fifteen times smaller time steps would have been needed to get a stable resolution. In fact the only constraining CFL here comes from explicit diffusion which is smaller than $\frac{1}{6}$ (3D CFL bound) due to small η value. So all these computations are stable with good conservation.

Computation box volume	$20 \times 20 \times 10\ \mu m^3$
Cilia length	$7\ \mu m$
Cilia radius	$200\ nm$
Initial mass fraction	$\alpha_0(x, y, z) = z - z_{min}$
Rheological law	$\phi(\alpha) = \mu_{ref} \left(1 + \frac{10}{1+exp(-(\alpha-6)/2)}\right)$
Mass diffusion	$\eta = 3 \times 10^{-13}\ m^2\ s^{-1} = 0.3\ \mu m^2\ s^{-1}$
Reference viscosity	$\mu_{ref} = 10^{-3}\ Pa\ s$
Cilia beating period	$0.25\ s$

Table 1: Simulation parameters for cilia beating

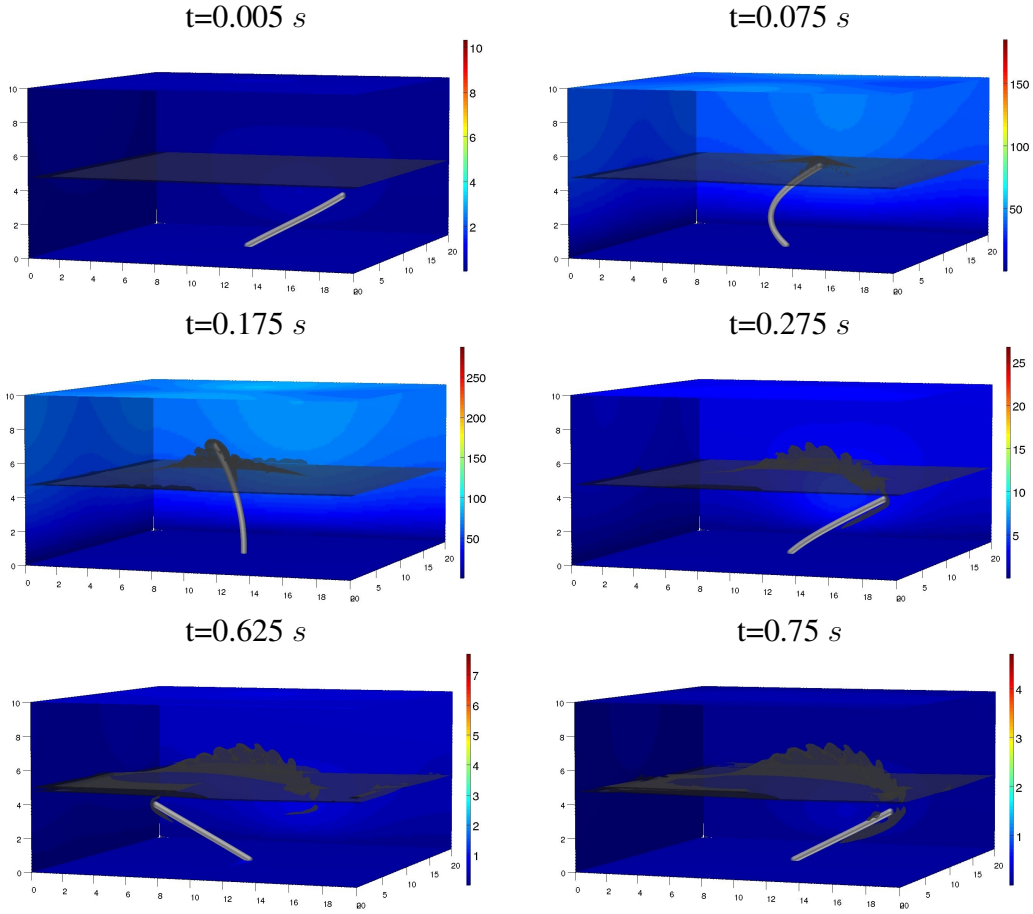

Figure 2: Beating along three periods of one cilium in a variable viscosity mucus at different times. Grey surface is a viscosity isosurface of level $4 \times 10^{-3}\ Pa \cdot s^{-1}$. At initialisation fluid is ten times more viscous at the surface (viscosity only depends on $\alpha(z)$) with strong gradients localised around cilia tips during recovery (with logistic function). Velocity norm is plotted on planes $x = 0\ \mu m$, $y = 20\ \mu m$, $z = 0\ \mu m$ (bronchial wall), and $z = 10\ \mu m$ (biofilm surface). Figures show velocity is more intense during effective stroke (when cilia beat from left to right, from distal to proximal airways) than during recovery (from right to left). Coupling between Stokes and advection-diffusion equation generates strong non-linear effects. Resolution presented is $256 \times 256 \times 128$. Legend is using micrometers as length unit.

On figure 3 the magnitude of surface velocity x component (direction from distal to proximal airways) is plotted (dash line). During recovery velocity is negative whereas it is positive during

effective stroke but magnitude is more important during stroke due to asymmetric beating and viscosity gradients. Thus average velocity over the cycle is globally positive which means mucociliary clearance is effective. Parameters were chosen according to an healthy mucus and results of $2.63\ cm \cdot s^{-1}$ is compatible with medical observations [18].

Figure 2 is presenting some snapshots at six different times of simulation. In grey an isosurface of viscosity is displayed and magnitude of velocity norm is presented on four computation box surfaces. At the beginning of simulation viscosity is stratified with respect to a logistic function of z and is then mixed with cilium beating. Mucociliary clearance appears efficient on this pictures as the furrow created by cilium in the isosurface is globally moving forward even if it is doing round trips.

3.3 Simulation of mucus propulsion around a simplified epithelium ciliated cell

The cell used for this simulation is composed of nine cilia organised as a 3 by 3 pattern. Cilia radius remains $200\ nm$ and a distance of $1\ \mu m$ is separating two adjacent cilia. Simulation parameters are identical as for previous simulation (see table 1). Remark about CFL condition of previous section remains valid here as velocity generated by nine cilia is more important than for one cilium.

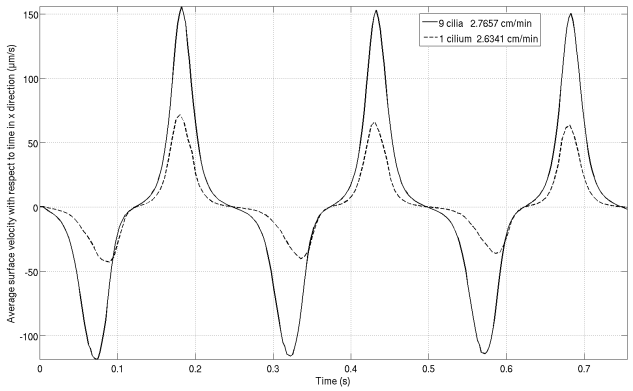

Figure 3: Average velocity u_x on the surface of biofilm for two configurations: a single cilium (dash line) and nine cilia (solid).

Figure 3 is also presenting average surface velocity on film surface for this 9 cilia simulation (solid line). Velocity magnitude is more important than in the case of a single cilium. But as magnitude is more important for both recovery (negative velocity) and stroke (positive) the average velocity over four periods is only 5% greater than for a single cilium: $2.74\ cm \cdot min^{-1}$. More cilia are generating a more important mucus motion inducing a more effective mucociliary clearance.

Figure 4 is presenting snapshots of the nine cilia simulation at same instants as figure 2. One clearly sees velocity generated by this cell is much more important than with single cilium. As cilia motion is governed by a 1D PDE computations of cilia motion and velocity $\bar{u}$ are negligible. Thus computations for a nine cilia cell are not greater than for a single cilium.

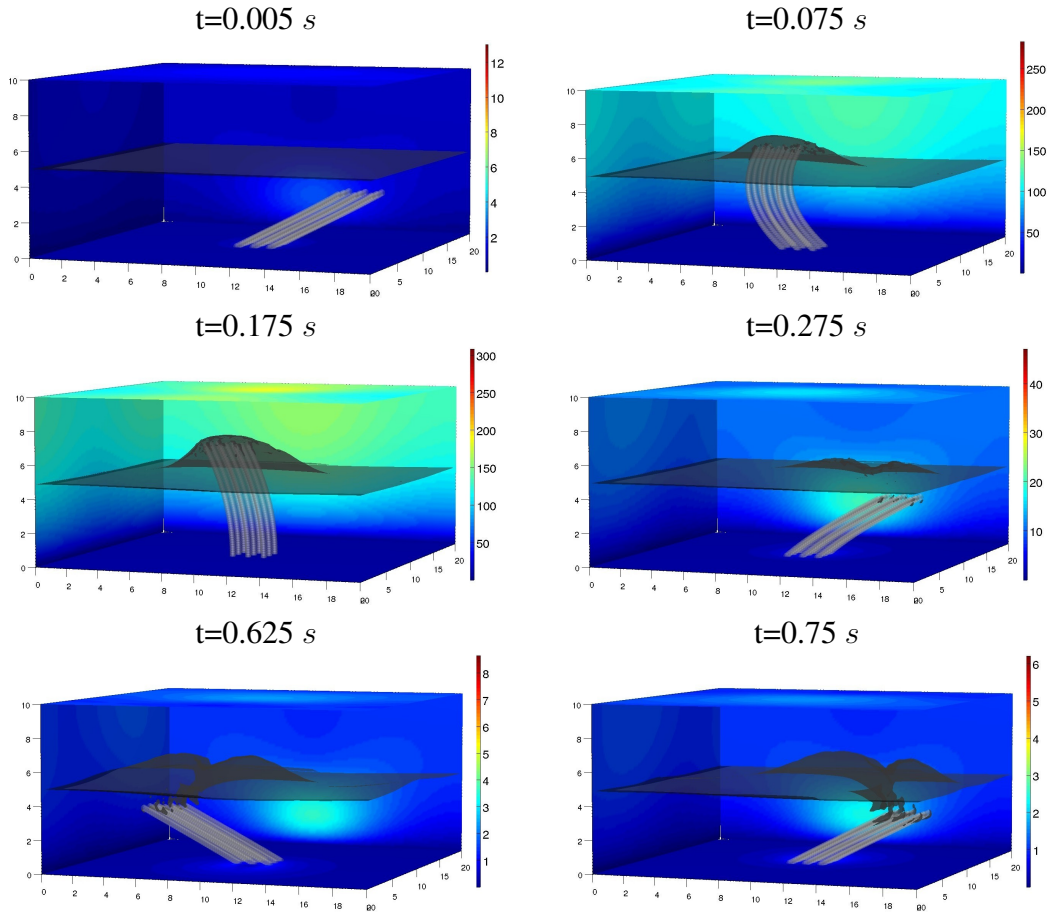

Figure 4: Beating along three periods of a 9 cilia epithelium cell in a variable viscosity mucus at different times. Grey surface is a viscosity isosurface of level $4 \times 10^{-3}\ Pa \cdot s^{-1}$. At initialisation fluid is ten times more viscous at the surface (viscosity only depends on $\alpha(z)$) with strong gradients localised around cilia tips during recovery (with logistics function). Velocity norm is plotted on planes $x = 0\ \mu m$, $y = 20\ \mu m$, $z = 0\ \mu m$ (bronchial wall), and $z = 10\ \mu m$ (biofilm surface). Figures show velocity is more intense during effective stroke (when cilia beat from left to right, from distal to proximal airways) than during recovery (from right to left). Coupling between Stokes and advection-diffusion equation generates strong non-linear effects. Resolution presented is $256 \times 256 \times 128$. Legend is using micrometers as length unit.

4 CONCLUSIONS

A coupled equation system has been proposed to model a highly 3D viscous flow with a variable viscosity and a one-way fluid-solid interaction. It consists in the classical linear Stokes problem with a penalization term but variable viscosity is inducing a non linearity. An iterative process based on solving Helmholtz and Laplace problems has been developed to consider this non linearity and the incompressibility condition without assembling matrix and solving linear systems. Coupling between velocity and viscosity is assumed with an advection diffusion equation of mass fraction α where advection is dominating. Viscosity is directly depending on this mass fraction such that $\mu = \phi(\alpha)$. A splitting strategy is used to solve separately effects of advection and diffusion. Advection is computed with a Lagrangian method which enables to transform PDEs into a set of ODEs so that no CFL condition is constraining time steps. As convection is dominating, diffusion is computed with an explicit straightforward algorithm which remains stable and not constraining time steps. These numerical strategies

allow to perform simulations with a fine spatial discretisation (here up to 512^3) over large time scales on a single CPU.

This algorithm is particularly adapted to compute mucus flow in the human lung at an epithelium cell scale. In fact microfluidics dimensions of the flow are inducing the use of Stokes flow and complexity of mucus film composition can be modelled with a variable viscosity flow depending of mass fraction. Motion of cilia is computed with a 1D advection equation posed along a parametrised curve. Adapted boundary conditions are generating oscillations and advection field (which is not velocity generated by Stokes flow) is approximating polymerisation. Simulations have been presented for a single cilium and for a cell composed of nine cilia over several beating periods and the global displacement of film surface shows that mucus is flowing in the direction of trachea at rates compatible with biological observations. This phenomena is so called mucociliary clearance.

In the future the model will be completed to consider the non Newtonian characteristic of mucus gel which is both viscoelastic and shear-thinning. It means more non linearities have to be introduced in the conservation of momentum equation of Stokes problem. These modifications should not improve computation cost since fixed-point algorithm is still multi-criterion. Finally this model will be intensely used to underline dominating mechanism of mucociliary clearance and lack of propelling considering lung pathologies as cystic fibrosis disease and aerosol therapy.

Acknowledgment

This work is supported by ANR Grant BioFiReaDy, under the contract number ANR-2010-JCJC-0113-01.

REFERENCES

[1] J. Adams: MUDPACK: Multigrid Fortran Software for the Efficient Solution of Linear Elliptic Partial Differential Equations, *Appl. Math. Comp.*, 34 (1989), 113-146

[2] P. Angot, C.-H. Bruneau and P. Fabrie: A penalization method to take into account obstacles in incompressible viscous flows, *Numer. Math.*, 81 (1999), 497-520

[3] J. T. Beale and A. Majda: Rates of convergence for viscous splitting of the Navier-Stokes equations, *Math. Comp.*, 37 (1981), 243-259

[4] F. Boyer, P. Fabrie, Eléments d'analyse pour l'étude de quelques modèles d'écoulements de fluides visqueux incompressibles, Springer Verlag, 2006

[5] R. Chatelin, P. Poncet: A particle method for moving bodies in a 3D Stokes flow with variable density and viscosity *Submited*, 2012

[6] G.-H. Cottet and P. D. Koumoutsakos: Vortex methods, theory and practice, Cambridge University Press, 2000

[7] G.-H. Cottet and P. Poncet: Advances in direct numerical simulations of three-dimensional wall-bounded flows by Particle in Cell methods, *J. Comp. Phys.*, 193 (2003), 136-158

[8] R. Cortez: The method of regularized Stokeslets, *SIAM Journal of Scientific Computing*, 23:4 (2002), 1204-1225

[9] T. Damy, P-R. Burgel, J-L. Pepin, P-Y. Boelle, C. Cracowski, M. Murris-Espin, R. Nove-Josserand, N. Stremler, T. Simon, S. Adnot, B. Fauroux: Pulmonary acceleration time to optimize the timing of lung transplant in cystic fibrosis, *Pulmonary Circulation* 2:1 (2012), 7583

[10] J.V. Fahy and B.F. Dickey: Airway mucus function and dysfunction, *New England Journal of Medicine*, 363 (2010), 2233-2247

[11] J.L. Guermond, P. Minev, J. Shen: An overview of projection methods for incompressible flows, *Comput. Methods in Appl. Mech. Engrg.*, 195 (2006), 6011-6045

[12] J. J. Monaghan: Extrapolating B-Splines for interpolation, *J. Comp. Phys.*, 60 (1985), 253-262

[13] M. El Ossmani and P. Poncet: Efficiency of multi-scale hybrid grid-particle vortex methods, *SIAM MMS*, 8:5 (2010), 1671-1690.

[14] P. Poncet: Analysis of direct three-dimensional parabolic panel methods, *SIAM J. Numer. Anal.*, 45:6 (2007), 2259-2297

[15] D.J. Smith, E.A. Gaffney and J.R. Blake: Discrete cilia modelling with singularity distributions: application to the embryonic node and the airway surface liquid, *Bulletin of mathematical biology*, 69:5 (2007), 1477-1510

[16] P. Swarztrauber and R. Sweet: Efficient FORTRAN Subprograms for the Solution of Elliptic Partial Differential Equations, *NCAR Technical Note-TN/IA*, 109 (July 1975)

[17] R. Sweet: A Parallel and Vector Variant of the Cyclic Reduction Algorithm, *SIAM J. Sci. and Stat. Comp.*, 9 (1988), 761-766

[18] M. Thiriet: Tissue Functioning and Remodeling in the Circulatory and Ventilatory Systems (Vol. 5), Series Biomathematical and Biomechanical Modeling of the Circulatory and Ventilatory Systems, Springer, New York, 2012